Int. J. Heat Mass Transfer. Vol. 25, No. 7, pp. 1043–1058, 1982
Printed in Great Britain

0017-9310/82/071043-16 $03.00/0
Pergamon Press Ltd.

THERMOHYDRAULIC CHARACTERISTICS OF SINGLE RODS WITH THREE-DIMENSIONAL ROUGHNESS

L. MEYER
Institut für Neutronenphysik und Reaktortechnik Kernforschungszentrum,
75 Karlsruhe, Federal Republic of Germany

(*Received* 29 *June* 1981)

Abstract—An investigation has been carried out into the heat transfer and friction characteristics of three-dimensional roughnesses consisting of uniformly distributed protrusions with sharp edges. The results of measurements of the velocity and temperature distributions in rough annuli are used to analyze data obtained from measurement of the pressure drop and heat transfer on seven single rods with different roughnesses contained in up to four smooth outer tubes. The results show that three dimensional roughnesses, within a certain range of rib parameters, produce higher friction factors and Stanton numbers than two-dimensional roughnesses. For such roughnesses the law of the wall does not hold as regards velocity and temperature distributions. Correlations for determination of friction factors and Stanton numbers in different annuli are given in the paper. A simple method of transforming the Stanton number measured in an annulus into an arbitrary annular cross section is presented.

NOMENCLATURE

A, cross-sectional flow area [m^2];
$A_{r,s}$, slope of the logarithmic velocity profile;
A_H, slope of the logarithmic temperature profile;
b, width of the ribs [m];
c_p, specific heat at constant pressure [$W\,s\,kg^{-1}\,K^{-1}$];
D_h, hydraulic diameter [m];
d, diameter of rod [m];
e, length of the rib in the circumferential direction [m];
f, friction factor $2\tau/\rho u^2$;
G, parameter in the logarithmic temperature profile for rough surfaces;
g, gap between two ribs in the circumferential direction [m];
h, height of the roughness ribs [m];
h^+, dimensionless height of the rib or roughness Reynolds number hu^*/ν;
Nu, Nusselt number;
p, pitch of the roughness ribs [m];
P, pitch of the rods in a bundle [m];
Pr, Prandtl number;
q, heat flux [$W\,m^{-2}$];
r, radius [m];
R, parameter in the logarithmic velocity profile for rough surfaces;
Re, Reynolds number, uD_h/ν;
Re^*, roughness Reynolds number transformed by equation (22);
St, Stanton number, $\alpha/(\rho u c_p) = Nu/RePr$;
St_0/St_{01}, Stanton number reduced by equations (18) and (21);
T, temperature [K];
t^+, dimensionless gas temperature, $(T_W - T)\rho c_p u^*/q$;
u, gas velocity [$m\,s^{-1}$];
u^*, friction velocity, $\sqrt{(\tau/\rho)}$ [$m\,s^{-1}$];
u^+, dimensionless velocity, u/u^*;
x, axial length starting at the beginning of rod heating [m];
y, radial distance from rough surface [m];
$\hat{y}$, radial distance of zero shear stress plane from wall [m];
y^+, dimensionless radial distance from the wall, yu^*/ν.

Greek symbols

α, convective heat transfer coefficient [$W\,m^{-2}\,K^{-1}$];
α, r_1/r_2;
β, r_0/r_2;
γ, r_0/r_1;
ν, kinematic viscosity [$m^2\,s^{-1}$];
ρ, density of the gas [$kg\,m^{-3}$];
τ, shear stress at the wall [$N\,m^{-2}$].

Subscripts

B, bulk or total of the annular cross-section;
1, inner rough zone of channel;
2, outer smooth zone of channel;
W, wall;
0, zero shear position or normalized;
R, reduced for temperature effect;
r, rough;
s, smooth.

INTRODUCTION

ROUGHENING a surface improves the heat transfer to a fluid flowing past it. There are many possible shapes of roughness such as regularly spaced ribs of any shape

provided at any angle to the flow. These are called 'two-dimensional roughnesses'. A uniform or random distribution of single bodies or protrusions of any shape on a surface is called a 'three-dimensional roughness'. The first artificial roughness which was investigated extensively by Nikuradse [1], the so-called sand-grain roughness, belongs to this category.

This work is concerned with the investigation of the heat transfer and friction characteristics of three-dimensional (3-dim.) roughnesses consisting of uniformly distributed protrusions with sharp edges.

A great number of investigations of heat transfer from rough surfaces were performed with two-dimensional (2-dim.) roughnesses. Thus the optimum shape of roughness is known quite well for this category.

The index of merit is the ratio $(St/St_s)^n/(f/f_s)$, generally called the 'thermal performance' of a roughness. The magnitude of the exponent n depends on the system in which rough surfaces are provided. For gas-cooled reactors a value of $n = 3$ is widely accepted. For 2-dim. roughnesses it was found that a roughness yielding high friction factors produces also a high thermal performance [2–5]. The optimum pitch to height ratio of the roughness ribs lies between 7 and 9. Some controversy exists on the optimum shape of the roughness edges, the angle of the leading and trailing edges and the angle of the ribs with respect to the flow direction [6]. Several investigators found better performances with helically ribbed surfaces than with transverse ribs [7–9].

An early investigation of heat transfer with 3-dim. roughness did not result in better thermal performances compared to 2-dim. roughnesses [10]. This was because of the too large spacing between the individual roughness bodies, as is now known from a systematic study on the flow resistance of 3-dim. roughnesses [11].

From hydraulic research work on the flow in open channels it has been known for a long time that some 3-dim. roughnesses produce a higher flow resistance than 2-dim. roughnesses [12, 13]. It was therefore assumed that these 3-dim. roughnesses also have a higher heat transfer capability than 2-dim. roughnesses. Preliminary results of experiments on two different 3-dim. roughnesses performed at my laboratory were reported in [14, 15]. These results confirmed the assumption of a superior thermal performance, however, it was difficult to correlate the results in terms of the roughness parameters of the non-dimensional velocity and temperature distributions, the so-called R- and G-functions. Therefore, an experimental program was performed to study the thermo-hydraulic behavior of geometrically well-defined 3-dim. roughnesses.

The investigations had two objectives. On the one hand, the dependency of the friction factor and heat transfer coefficient on the roughness geometry should be clarified with the aim of finding an optimum.

On the other hand, the problem of the 'transformation' of experimental results for rough single rods in smooth tubes into clusters of rods should be solved. One of the various transformation methods assumed the validity of 'universal' velocity and temperature profiles over rough and smooth walls [16]. Thereby it is possible to separate the effect of the rough wall from that of the smooth wall and to determine the friction factor and heat transfer coefficients in channels with different geometries. Recent measurements of velocity distributions in various rough channels [17–20], however, indicate that the velocity profile is not 'universal', i.e. the slope changes with the roughness and channel geometry. Therefore, velocity and temperature profiles over 3-dim. roughnesses were measured first. This paper concentrates on the pressure drop and heat transfer experiments at single pins with three-dimensional roughness but it also reviews the experiments which were performed at our laboratory, in order to find the optimum roughness geometry and determine velocity and temperature profiles. The number of experimental data is so great that only the main results will be mentioned here. All the results are presented in listings and diagrams in a number of previously published papers [11, 21–26].

CHANGE OF FRICTION FACTOR WITH ROUGHNESS GEOMETRY

The geometry of a two-dimensional roughness with transverse rectangular ribs is defined by three parameters, the rib height h, the width b and the axial spacing or pitch p. A three-dimensional roughness has two additional parameters, the length of a rib e and the lateral gap g (Fig. 1). provided the ribs are arranged in a symmetric pattern. A potential technique to find the optimum parameter configuration was proposed by Lewis [27], who developed a method to predict by analysis the momentum and heat transfer characteristics of a roughness. His flow model required form drag coefficients of single roughness elements, separation lengths behind an element and the knowledge of the heat transfer coefficient distribution. Although the experimental data from 2-dim. roughnesses were fairly well predictable by the method sufficient information was not available to calculate satisfactorily the behavior of 3-dim. roughnesses. Therefore, an experiment was performed in which the parameters p and g were systematically varied and the friction factors measured [11, 28]. The measurements were performed in a rectangular channel with variable aspect ratio. Besides the axial pressure drop, the velocity distribution and the force acting upon a single roughness rib were measured.

The most important result of this investigation is shown in Fig. 2. Here the friction factor based on the maximum velocity in the flow cross section is plotted versus a parameter describing the roughness density: $p/h(1 + g/e)$. These results are mean values of three measurements made for different Reynolds numbers in the high turbulent regime. The comparison with 2-dim.

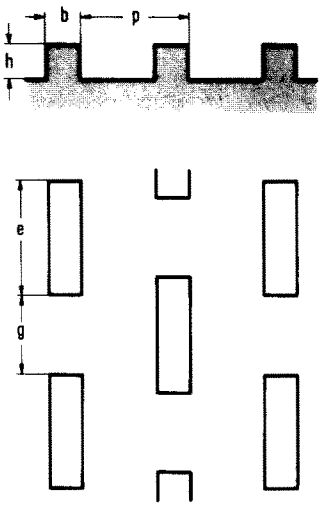

FIG. 1. Parameters of a 3-dim. roughness.

roughnesses ($g/e = 0$) shows the high friction of certain 3-dim. roughnesses. The maximum is reached for configurations where the lateral gap is approximately as wide as the length of the element and the p/h-ratio is 2.5. Due to the shorter 'dead water' region behind a single element compared to those behind a rib of a 2-dim. roughness, the roughness elements can be arranged closer in the axial direction and thus produce more total drag.

In the same test rig the form drag coefficients of single elements and the separation lengths upstream and downstream of an element were measured [11]. This information was used to calculate the friction factor by Lewis' method. The results did not agree with friction factors determined from experimental data. Apart from the different behavior of the flow at single elements and at element arrays, the reason for the failure of this method is the assumption of a constant slope of the non-dimensional velocity profile. Measurements of the velocity distribution had shown that the slope differs from the hitherto assumed value of 2.5, especially for roughnesses with high friction factors. Thus Lewis' method cannot be expected to produce correct results for the heat transfer coefficient either.

VELOCITY AND TEMPERATURE PROFILES

As mentioned above, a method is needed to correlate friction and heat transfer data, extrapolate them to different roughness heights or transform measurements made in channels with both rough and smooth walls into channels with rough walls only. The assumption of 'universal' velocity and temperature profiles near smooth and rough walls has led to good results in many cases. For the dimensionless velocity distribution we have Nikuradse's law of the smooth wall

$$u^+ = A_s \ln y^+ + 5.5 \tag{1}$$

and for the rough wall

$$u^+ = A_r \ln y/h + R \tag{2}$$

with the slopes A_s and A_r being the same for both cases. For sufficiently high values of h^+ the parameter R was found to be constant for a given roughness, independent of the geometry of the flow channel. Integration of equation (2) over the flow cross section yields the friction factor.

By analogy with the velocity distribution Dipprey and Sabersky [29] introduced the non-dimensional temperature profile near rough walls

$$t^+ = A_H \ln y/h + G \tag{3}$$

and correlated their heat transfer data in terms of the

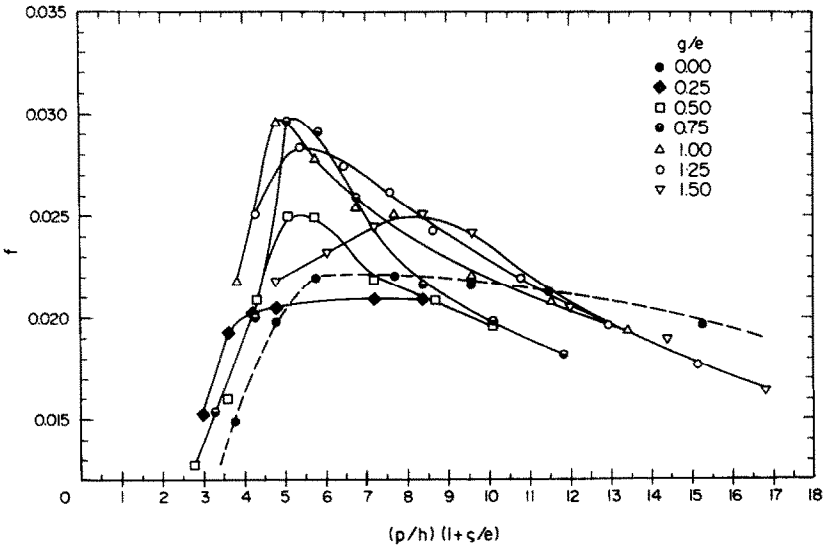

FIG. 2. Friction factor of 3-dim. roughness, $e/h = 4$.

parameter G. Contrary to f- and St-correlations, the R- and G-functions allowed to extrapolate easily measured data to different relative roughness heights and even to different channel shapes, although the latter extrapolation was always subject to doubts and controversy.

The universal velocity profiles were used first by Maubach [16] to separate the effects of smooth and rough walls in single-pin annulus experiments. To separate the two zones it is assumed that the plane of zero shear stress is given by the intersection of the two velocity profiles originating at the respective walls. Assuming the validity of the temperature profile in the total cross section of an annulus, Dalle Donne and Meyer [5] were able to calculate the temperatures in the two zones. A comprehensive description of these and other methods is given in refs. [5, 17].

The weak point when using universal profiles is the uncertainty of their universality. It is well known that they are not valid close to, or far from the wall. It is not known what is the influence of the curvature of the wall, and only recently it was found that certain types of roughnesses change the slope considerably.

Aytekin [17] found different slopes in rough pipes and annuli for both the logarithmic velocity and temperature profiles, with the ratio A_H/A_r being similar in different geometries. Whitehead [18, 30] found the slope A_r to be a function of the p/h-ratio of the two-dimensional square ribs in pipe flow. An additional variation of the slope A_r due to different relative roughness heights $h/\hat{y}$ was found by Baumann [19] in a rectangular closed water channel. An investigation with air in a parallel plate channel indicated a direct relation between the slope of the logarithmic velocity profile and the drag of the 2-dim. roughness [11, 20]. Velocity profiles with low slopes ($A_r < 2.5$) were found over roughnesses with high friction factors. This investigation also showed the importance of the proper definition of the origin of the velocity profile at the rough wall if measurements by different authors are to be compared with each other.

Measurements with 3-dim. roughnesses in the same channel showed even lower slopes than the lowest slope from 2-dim. roughnesses [23]. This corresponds to higher friction factors measured.

This investigation for roughnesses with extremely high friction factors underlines some points, some already known from 2-dim. roughnesses. In experiments with one wall rough and the opposite wall smooth, the displacement of the position of zero shear from the position of maximum velocity in the direction of the smooth wall was very large. The flow in the smooth zone is significantly affected by the rough wall and so is the flow in the rough zone by the presence of the smooth wall. The velocity distribution for different channel widths is very different. It was found in earlier investigations that the friction factor of the smooth zone increases by the presence of the opposite rough wall. Now it was found that the friction factor in the rough zone, too, is different depending whether it is adjacent to a 'smooth zone flow' or a 'rough zone flow'. Therefore, an accurate transformation of single-pin results into rod clusters is no longer possible unless this difference is taken into account. This might have been true for 2-dim. roughnesses also, but the errors were probably less serious than the other inaccuracies involved. For 3-dim. roughnesses the error may exceed 10% with relative roughness heights $h/\hat{y}_r + = 0.1$.

Subsequent measurements of velocity and temperature distributions in an annular geometry with rough rods [24] showed that the slopes of the logarithmic profiles also vary with the Reynolds number Re and h^+, respectively. Most of the apparent variations of R known from evaluations of pressure drop measurements with 2-dim. roughness [5] are in fact due to a variation of the slope A_r which hitherto has been taken to be constant. With falling values of h^+ the slope A_r increases. The same is true for the slope of the temperature profile A_H.

The temperature profiles deviate from a logarithmic straight line at great distance from the heated rough wall. These deviations as well as the deviations of the velocity profile from a straight line must be taken into account if these parameters are to be used to calculate friction and Stanton numbers by integrating equations (2) and (3) over the flow cross section. This is done by determination of A_r and A_H through integration of the measured data and complying with certain boundary conditions, rather than taking them directly from semi-logarithmic plots.

The conclusion of the measurements, especially for 3-dim. roughnesses with high friction factors, is that there is no 'universal' velocity or temperature profile. A straight portion exists only in a very limited range of distances from the wall or in some cases not at all. If equations (1)–(3) are still used for calculating friction factors and Stanton numbers, the parameters A_r and A_H determined by integral quantities should be functions of the type of roughness and channel geometry and of the relative roughness height. The magnitude of errors arising if constant slopes ($A_r = A_H = 2.5$) are used, depends on the same parameters. Large errors (> 5–10%) occur at low Reynolds numbers or roughnesses with high drag and high relative roughness heights, respectively.

The application of a 'universal' eddy diffusivity distribution is not thought to yield substantially better results, since it is dependent on the same parameters.

PRESSURE DROP AND HEAT TRANSFER EXPERIMENTS

Experimental apparatus

The experimental apparatus and the experimental techniques used are similar to those used for the experiments on 2-dim. roughnesses [5]. The tests are performed in an annular test section with a single rough rod supported concentrically in a smooth outer tube. The rod consists of a tube of stainless steel. It is

heated directly by alternating current and cooled by air at pressures between 1 and 5 bar. The mass flow rate is determined by one of various orifice plates which are placed in parallel and have been calibrated to an accuracy better than 1% for the optimum range of application. The pressure drop along the test section was measured by up to 16 static pressure taps provided in the outer smooth tube. The absolute and differential pressures were measured by five pressure transducers of the capacitance type with an accuracy better than 1% in the whole range between 1 and $10^6\,N\,m^{-2}$. Temperatures were measured by sheathed Chromel/Alumel thermocouples. Up to 20 thermocouples had been installed in the wall of the rough rod close to the rough surface with up to 4 at the same axial position in order to check for possible eccentricities in the annulus. Up to 26 thermocouples were inside the wall of the smooth tube which had been insulated to minimize heat losses. The gas temperatures at the inlet and at the outlet of the test section were measured by shielded thermocouples. These temperatures were checked by means of a heat balance between the electrical input power and the thermal power. Only runs with heat balances better than 5% were considered for the evaluation.

Experimental parameters

Two series of tests with different sizes of rough rods were performed. One series was performed with rods of 34 mm O.D. the other with rods of 8 mm O.D., which is similar to rods proposed for a Gas Cooled Fast Reactor. The heated length of the large rods was 2000 mm and that of the small rods 800 mm. The large rods were tested in four different smooth outer tubes of 40, 50, 70 and 85 mm I.D., respectively. No heated tests were run with the 40 mm outer tube. The small rods were tested in two outer tubes of 16 and 20 mm I.D., respectively.

Two basically different roughness shapes were tested. The first is similar to that shown in Fig. 1 (rods 10 and 12). It was manufactured by spark erosion which is an expensive procedure. Therefore, a geometry was sought which should show similar thermohydraulic characteristics but was also cheaper to produce. By machining threads into the rod surface with the same pitch, in both directions, a rhombic geometry as shown in Fig. 3 was obtained (rods 15, 16, 17 and 3). The roughness on the small rod No. 2 was obtained by machining an additional thread with a small pitch in such a way that the corners of the rhombus were cut away. This roughness shape (Fig. 4) is similar to the first (Fig. 1).

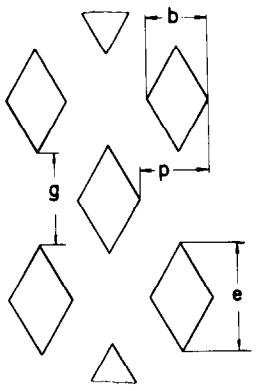

FIG. 3. Roughness geometry of rods 15, 16, 17 and 3.

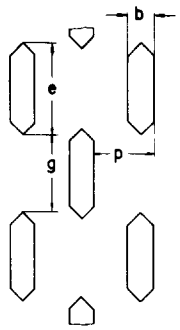

FIG. 4. Roughness geometry of rod 2.

The exact geometrical parameters are listed in Table 1 together with the radius of the rods which is defined volumetrically. For easy reference to the complete listings of the experimental data, the same numbers of the rods are retained as in Mayer and Neu.*

The Reynolds numbers covered by the experiments ranged from the laminar region to $Re = 3 \times 10^5$. Each rod was first tested without heating and then at up to three temperature levels, e.g. maximum wall temperatures of 150, 350 and 550°C.

EVALUATION

For the determination of the true surface temperature of the rough rods two corrections at the thermocouple readings were applied. Since the thermocouple junctions lie below the surface, the temperature reading is too high. A correction is made by taking into account the heat condution in the radial direction. Another correction is necessary to take into account the fact that the surface temperature is not constant between the ribs. This variation depends on the conductivity of the material of the rod and of the cooling gas, which was air, the temperature difference between the wall and gas, the heat flux and the roughness geometry. The maximum correction for this so-called 'fin efficiency effect' was only 4.7 K at the highest heat flux and wall temperature.

To calculate the heat transferred by convection from the rough rod to the gas, the heat transferred to the outer tube by radiation was subtracted from the

* There is an error in Table 1 of ref. [26], giving incorrect data for e and g for rods 2 and 3.

Table 1. Geometrical parameters of the rough rods

Rod	h	b	p	e	g	r_1
10	0.80	0.30	1.60	3.0	2.9	16.44
12	0.60	0.30	1.60	3.0	2.9	16.38
15	0.39	2.2	4.25	3.55	3.7	16.01
16	0.75	2.2	4.25	3.55	3.7	16.15
17	1.15	2.2	4.25	3.55	3.7	16.31
2	0.20	0.25	0.61	1.16	1.12	3.84
3	0.20	0.58	0.61	1.16	1.12	3.87

electrically generated heat. The emissivity had been determined in an evacuated test section.

In the calculation of the friction factor the pressure drop due to acceleration of the gas was taken into account. With respect to the heated tests the measured pressure differences were corrected for the different air densities within the test section and within the connection lines leading to the pressure transducer. This buoyancy effect was quite large at low mass flow rates. The evaluation of friction and heat transfer coefficients and the transformation procedure were performed with local data along the test section. Mean values were obtained by averaging the local results over an axial section where the results were relatively constant.

FRICTION FACTOR

From the bulk of data some examples will be shown here. All the results are listed in refs. [25, 26].

The friction factor of the entire annulus for rod 12 in four different outer smooth tubes is shown in Fig. 5. These are results from isothermal runs. Above a Reynolds number $Re = 2 \times 10^4$ all friction factors are constant. This means that the contribution of the friction at the smooth wall to the total friction is very small. For a roughness with a lower drag the bulk friction factor decreases with the Reynolds number getting higher. This is the case for rod 15. The roughness of rod 12 showed the highest friction factors for a fixed h/D_h-ratio. The ratio of pitch to height (p/h) of this roughness lies near the optimum in Fig. 2.

A transformation must be used to calculate the friction factors applicable to the inner 'rough' zone of flow which is bounded by the surface of zero shear and the rough surface of the rod. The transformation method used is based on the assumption of universal dimensionless velocity profiles and was developed by Maubach [16] and subsequently refined by Dalle Donne and Meyer [5]. Two laws of the wall for the velocity profiles starting from both walls of the annulus are assumed and the intersection of the profiles is interpreted as the zero shear position. The slope of the velocity profile starting from the rough wall was assumed to be $A_r = 2.5$, while the slope of the profile in the smoother outer zone is varied ($2.35 \leq A_s \leq 2.50$) to take into account the empirical friction factors of the smooth zone evaluated by Warburton [31]. The result of this transformation is the friction factor of the rough zone f_1, the width $\hat{y}$ of the velocity profile or the distance from the wall to the position of zero shear, and the roughness parameter R.

For rod 12 the parameter R evaluated with $A_r = 2.5$ is shown in Fig. 6. If the universal velocity profiles were valid in the entire flow cross sections of the two zones regardless of the size of the outer tube, the R-parameter should be the same for all four test sections. In fact, they are different by more than one point. This is true for all large rough rods. The differences are such that no correlation for R can be found. Since it is known that the slope A_r is not a constant, this result is not surprising. There is, however, no general correlation of A_r for the large variety of 3-dim. roughnesses. As mentioned above, it was found for 2-dim. and some 3-dim. roughnesses that the slope A_r decreases with increasing relative roughness height and with increasing friction factor. This was found for high Reynolds numbers and high values of h^+, respectively. For lower values of h^+ the slope A_r was found to increase again. This variation of A_r can be described by

$$A_r = C_1 + C_2/\log(h/\hat{y}_r) + C_3/\log h^+. \quad (4)$$

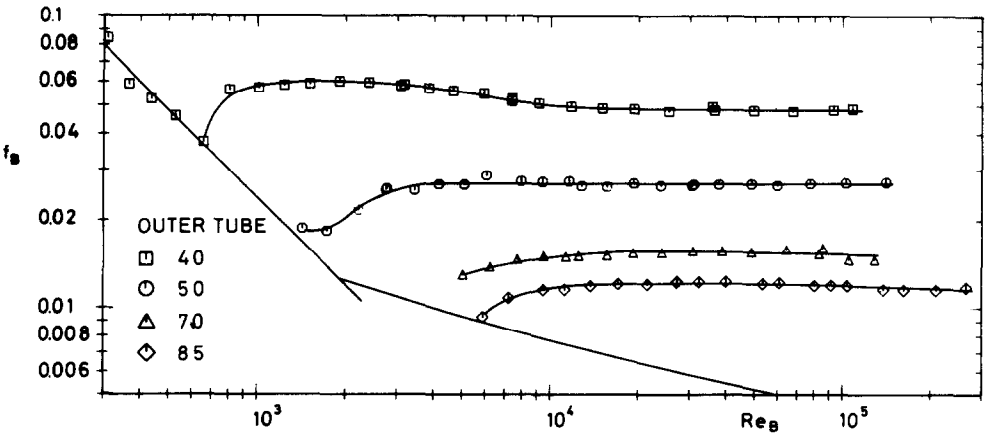

FIG. 5. Bulk friction factor for rod 12 in four different outer tubes.

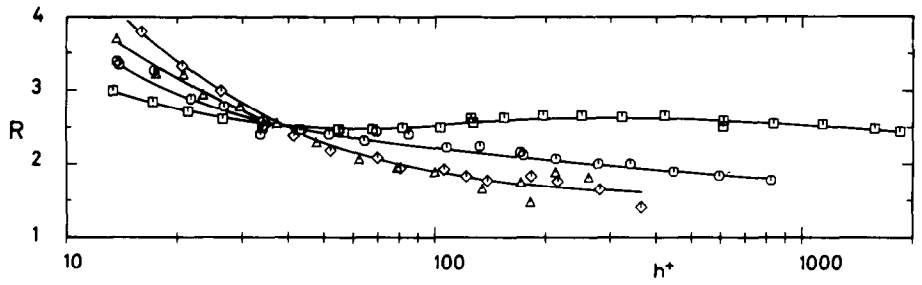

FIG. 6. Roughness parameter R for rod 12 evaluated with $A_r = 2.5$ (symbols as for Fig. 5).

For the determination of the constants C_i one can use a method first proposed by Hodge *et al.* [32]. The relation between the transformed friction factor f_1, the slope of the velocity profile A_r and the roughness parameter R valid for an annulus can be written as

$$(2/f_1)^{1/2} = A_r[\ln \hat{y}/h - \tfrac{1}{2} - 1/(2 + \hat{y}/r_1)] + R. \quad (5)$$

Figure 7 shows a plot of $(2/f_1)^{1/2}$ versus $\ln \hat{y}/h - \frac{1}{2} - 1/(2 + \hat{y}/r_1)$ with a Reynolds number $Re_1 = 10^5$ for the four large test sections.

If the law of the wall [equation (2)] held for all test sections within the flow in the 'rough' zone, the data for one rough rod in different outer tubes should fall on a straight line having the slope A_r. The intersection of this line with the ordinate would be R, a constant value for all outer tubes.

If the results obtained are joined by a line, it is seen that its slope varies. The slope decreases with increasing relative roughness height (smaller values at the abscissa). Lines can be drawn with constant slopes (constant A_r) through the points and get a variable R (different intersection with the ordinate for each point) or draw a line through a fixed value on the ordinate (constant R) and the various points and get variable slopes A_r. The first lines with a slope $A_r = 2.5$ yield the R-functions shown in Fig. 6. The second method was used in the following manner. In order to limit the number of correlations, equation (4) was applied for all test sections. The constants C_1 and C_2 were de-

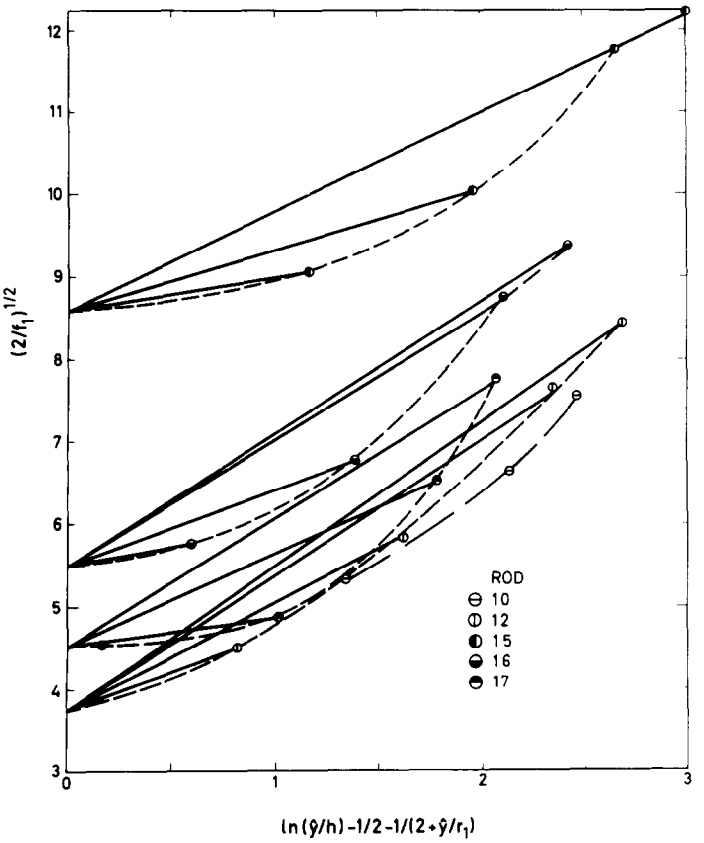

FIG. 7. Determination of the slope A_r by the method of Hodge *et al.* [32] ($Re_1 = 10^5$).

Table 2. Roughness parameters of the velocity profile, and friction factors evaluated for $h/\hat{y} = 0.065$ and $h^+ = 200$

Rod	C_1	C_2	C_3	R	for $h^+ >$	f_1
10	1.7	1.3	2.0	3.80 ± 0.20	30	0.047
12	1.7	1.3	2.0	3.75 ± 0.25	15	0.048
15	2.2	1.65	0.1	8.40 ± 0.30	20	0.020
16	2.95	2.3	0.8	5.50 ± 0.25	30	0.031
17	2.2	2.3	3.0	4.55 ± 0.25	100	0.035
2				4.30 ± 0.25	20	0.040
3				5.20 ± 0.25	20	0.032

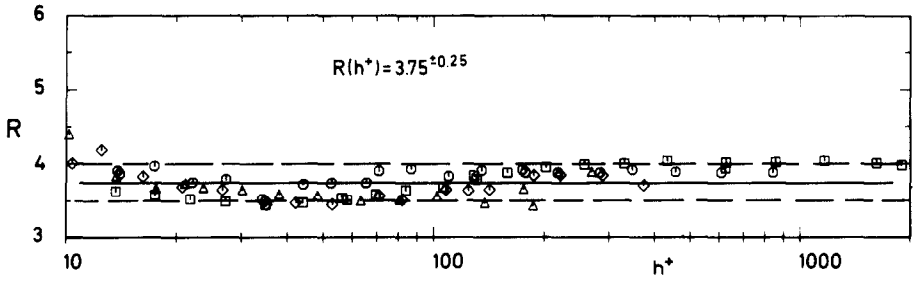

FIG. 8. Roughness parameter R for rod 12 evaluated with variable A_r (symbols as for Fig. 5).

termined from Fig. 6 in an approximation procedure. The constant C_3 was determined with the condition that R should be constant with the variable h^+. The constants for all large rods are listed in Table 2.

The transformation procedure was performed with a variable slope of the smooth velocity profile (A_s). The equation for A_s was found in a rectangular channel [11, 20]

$$A_s = 2.55 + 0.4/\ln\{0.1h/[r_2(1-\beta)]\}. \quad (6)$$

The R-values, determined with A_r and A_s by equations (5) and (6), are shown in Fig. 8 for rod 12. They are constant in a wide range of h^+ with a small amount of scatter. This is true for all rods, since the small rods were not tested in more than two outer tubes, the constants in equation (4) could not be determined. Therefore, the transformation of these experiments was performed with the constants of rods 10 and 12.

With different assumptions about the slopes of the velocity profiles the transformation produces different transformed friction factors. The position of the zero shear stress, denoted by $\hat{y}$, is different, too. The transformed friction factors f_1 for the rough zone evaluated with variable slopes A_r and A_s are plotted in Fig. 9. Also shown are lines which represent the results of a transformation with a constant $A_r = 2.5$ and a variable A_s. The differences are not such that a different transformation can change the trend of the curves in Fig. 7. The transformation with variable slope A_r gives generally lower friction factors f_1 and higher values f_2. The maximum differences occur in the small flow cross sections where the deviation of the slope A_r from 2.5 is greatest.

For small outer tubes (40 mm), which means great relative roughness heights variable A_r gives approximately 5% smaller friction factors (f_1) and 5% greater $\hat{y}$ values. In the 50 mm outer tube these differences are approximately 3% in both cases. In the 70 and 85 mm outer tubes the difference for the friction factor is less than 1% and approximately 3% for $\hat{y}$. These numbers are true for all test sections with small deviations in some cases, which depend also on the Reynolds number. The magnitude of the differences might not justify to apply variable slopes A_r since it is less than 3% for flow channels usual in reactor geometry. If, however, R-functions are to be used for the calculation of friction factors, a reliable correlation is needed for R, which is valid in the whole parameter field; otherwise the errors might become substantial. This is easier to realize with the variable A_r. Since measurements of the velocity distribution indicated variable slopes according to equation (4), the transformation using these can be expected to furnish more exact results. With equations (4) and (5) and the constants from Table 2, friction factors can be calculated for an arbitrary flow cross section within the limits of the tested ranges. It should, however, be kept in mind that the magnitude of the errors cannot be stated for other channel geometries than annuli. As mentioned before, the greatest errors are expected to arise for low Reynolds numbers and high relative roughness heights.

As a basis of comparison friction factors were calculated for a certain relative roughness height of $h/\hat{y} = 0.065$ and a roughness Reynolds number of $h^+ = 200$. These values are listed in Table 2. The rhom-

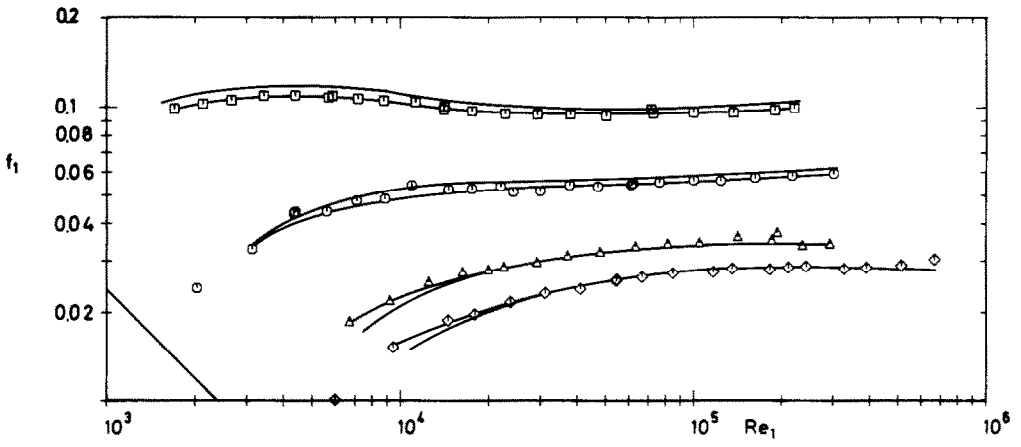

FIG. 9. Transformed friction factor for rod 12 in four different outer tubes (symbols as for Fig. 5).

bic roughnesses have generally lower friction factors than the rectangular ones. The friction factor of the small rod 2 is lower than those of the large rods 10 or 12. This is probably due to the larger relative rib width b/h of rod 2. For comparison the friction factor of transverse ribs with rounded edges would be $f = 0.022$ for the same $h/\hat{y}$-ratio [33].

The results of the heated tests indicated that the friction factor decreases with increasing temperature ratio T_W/T_B in the turbulent regime and increases in the laminar regime. The temperature effect in the laminar regime was discussed in [34] and can be eliminated if the bulk friction factor f_B is plotted versus Re_W, the Reynolds number being evaluated at a temperature T_W. This temperature is an average between the temperature of the inner rod surface and the outer smooth surface, the average being weighted over the two surfaces.

The transformed friction factors f_1 in the turbulent regime show a temperature effect similar to that of the bulk friction factor (Fig. 10(a), (b)). In a series of experiments with single rough pins cooled by various gases the temperature effect was reduced by plotting

$$f_{1R} = f_1 \left(\frac{T_W}{T_B}\right)^{0.29} \tag{7}$$

versus Re_{1W} [22]. The exponent was found to be the same for helium, nitrogen and air. This reduction was successfully applied in the present measurements for most cases. If one plots f_{1R} versus Re_{1W}, the results of the heated tests agree with those of the unheated tests at Reynolds numbers $Re_{1W} > 2 \times 10^4$ within the experimental error (Fig. 10(c)). In the transition region between fully rough flow and turbulent smooth flow no satisfactory correlation has been found up to now. For some test sections the correlation mentioned above also holds for Reynolds numbers below 2×10^4. No temperature effect was observed and consequently equation (7) could not be applied, for rod 17 at the highest Reynolds numbers and for the measurements at the small pins 2 and 3. Here a correlation of f_1 versus Re_{1W} was sufficient for the elimination of the temperature effect in the region $Re > 5 \times 10^3$. The reason for the different behavior is not known.

With reduced friction factors for heated tests a parameter R can be determined by equation (5) which is independent of the temperature ratio T_W/T_B. A temperature reduction of R, as proposed in [5], is not necessary under this condition. The parameter must be plotted versus a reduced roughness Reynolds number

$$h^+_{WR} = \frac{hu^*_{1R}}{\nu_W} = h^+_W \left[\left(\frac{T_W}{T_B}\right)^{0.29}\right]^{1/2} \tag{8}$$

in order to correlate them in the region where they are not constant. The scatter in these plots for a test section at different temperature levels is similar to the scatter of the results for one rod in different outer tubes.

STANTON NUMBER

The Stanton number St_B was determined from the convective heat transfer coefficient between the rough rod and the gas bulk in the entire flow cross section. Since the general correlation for gases is $St \sim Re^{0.2} Pr^{-0.6}$ all Staton numbers plotted were reduced by the factor $Pr^{0.6}$ for the Prandtl number effect. The Prandtl number effect cannot be investigated if only air is used as the coolant. Figure 11(a) shows the Stanton number versus the bulk Reynolds number for one test section. There is a strong effect of different T_W/T_B-ratios. The Stanton number decreases with increasing T_W/T_B.

This effect of the variation of the fluid properties with the temperature was taken into account by an exponent of the temperature ratio T_W/T_B according to Petukhov *et al.* [35]

$$\frac{Nu}{Nu_0} = \left(\frac{T_W}{T_B}\right)^n \tag{9}$$

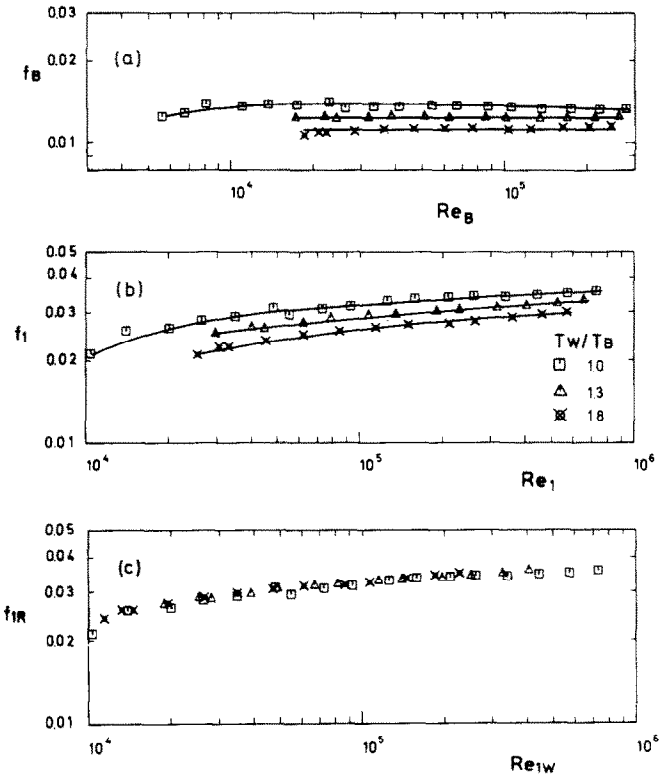

FIG. 10. Friction factors of heated test for rod 10 in the 85 mm outer tube (a) bulk, (b) transformed and (c) reduced for the temperature effect.

with

$$n = 0.53n_\rho + \tfrac{1}{3}u_2 + \tfrac{1}{4}n_{cp} - \phi(x/D_h)n_\mu \log\left(\frac{T_W}{T_B}\right). \quad (10)$$

n_ρ, n_2, n_{cp} and n_μ are the exponents of the temperature variations of the fluid properties, e.g.

$$\frac{\rho}{\rho_0} = \left(\frac{T}{T_0}\right)^{n_\rho}. \quad (11)$$

The influence of the entrance effect on the exponent of the temperature ratio, $\phi(x/D_h)$, was modified compared with Petukhov's correlation to become

$$\phi\left(\frac{x}{D_h}\right) = 0.4\left(1 + \frac{x/D_h}{25}\right). \quad (12)$$

This method of reducing the temperature effect of the Stanton number was found to hold for different gases [22]. In this investigation it could also be shown that the entrance effect on the Stanton numbers of the roughened surfaces could be eliminated by reducing them with a correlation valid for the entrance effect on Stanton numbers in smooth tubes [36] based on the experimental data of Alad'yev [37]

$$\frac{St}{St_\infty} = 1 + 14\,Re^{-0.35}\log\left[K\left(\frac{x}{D_h}\right)^{-0.6}\right] \geq 1. \quad (13)$$

The factor K was changed from 10, valid for smooth

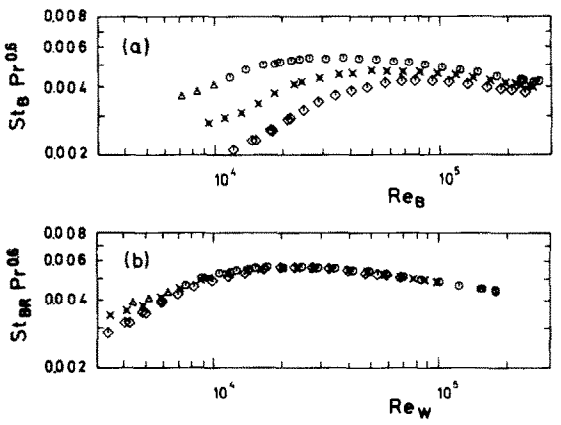

FIG. 11. Stanton numbers for rod 16 in the 85 mm outer tube, (a) vs bulk Reynolds number and (b) reduced for the temperature effect vs Reynolds number evaluated at wall temperature.

surfaces [37], to 4.35. This means that the entrance effect for rough surfaces is smaller than for smooth surfaces.

With the physical properties of air the exponent in equation (9) becomes for the present experiment

$$n = -0.243 - \phi\left(\frac{x}{D_h}\right)0.7 \log\left(\frac{T_W}{T_B}\right). \quad (14)$$

The reduced Stanton number $St_{BR}Pr^{0.6}$ plotted versus Re_W agrees with different T_W/T_B-ratios in most test sections down to Reynolds numbers $Re_W > 5 \times 10^3$ (Fig. 11(b)).

The bulk Stanton number should be transformed so that it applies to the case where the heat flux is zero at the zero shear stress position. Several methods have been proposed for this purpose. Methods based on the eddy diffusivity concept were developed by various authors [38–41]. The logarithmic temperature profile, first used by Dalle Donne and Meyer [5] to evaluate the temperatures in the rough and smooth zones and to determine the G-parameter, was used by Meyer and Rehme [22] to transform the Stanton numbers. This method is based on Hall's method [42], by which the heat flux distribution is transformed in such a way that there is no heat transfer at the surface of zero shear. The heat flux at the rough surface is maintained constant and a new temperature distribution is obtained. The method of Meyer and Rehme is, however, dependent on the validity of the universal temperature profile.

Since measurements of the temperature profile in rough annuli [24] had shown that the temperature distribution deviates from a straight logarithmic line, this method was refined by introducing variable slopes A_H for the temperature profiles. These slopes were determined from temperature traverses with the condition that integration of equation (3) over the entire channel or over the inner rough zone must yield the respective bulk temperatures T_B or T_1. As a result of this transformation method it was found that the ratio of the transformed Stanton number to the non-transformed number, St_1/St_B, was a simple function of the ratio of the flow cross sections, A_1/A_B [25]. The data points, St_1/St_B, plotted over A_1/A_B coincided on one curve for one rod tested in different outer tubes at different Reynolds numbers. Physical reasoning might point to a relation to the ratio of the mass flow rates, m_B/m_1, but since for turbulent flow the difference with respect to the ratio of the flow areas is small, this parameter is preferred for the sake of simplicity. The curve is approximated by the simple equation

$$\frac{St_1}{St_B} = \left(\frac{A_1}{A_B}\right)^{-0.3}. \quad (15)$$

With a transformation which is only a function of the ratio of the flow cross sections it is possible to transform the Stanton number into an arbitrary annular cross section. A proper flow cross section to be transformed is the annular cross section which is equivalent to the cross section of a tube with the radius r_1. The outer radius of this annulus is

$$r_0 = r_1\sqrt{2}. \quad (16)$$

The ratio of the flow cross section of the annulus and tube, respectively, and the original annulus is

$$\frac{A_0}{A_B} = \frac{r_1^2}{r_2^2 - r_1^2} = \frac{\alpha^2}{1 - \alpha^2}. \quad (17)$$

Thus, the measured bulk Stanton number reduced for the temperature effect, is transformed into a normalized Stanton number by

$$St_0 = St_{BR}\left(\frac{\alpha^2}{1 - \alpha^2}\right)^{-0.3}. \quad (18)$$

For a comparison of Stanton numbers, evaluated from measurements in different flow channels, the Reynolds number is not a suitable parameter. The conditions at the wall, which are governing the heat transfer process, are described best by the roughness Reynolds number h^+. In the case of a reduced Stanton number the parameter h^+_{WR} according to equation (8) should be applied.

In Fig. 12(a) the reduced Stanton numbers for rod 17 in three different outer tubes are plotted versus h^+_{WR}. Only data for $Re > 3000$ and $h^+ > 7$ are shown. At low h^+_{WR}-values the scatter is large due to an incomplete elimination of the temperature effect below $Re_W = 5000$. Figure 12(b) shows all data transformed into St_0 by equation (18). They lie on one curve with the amount of scatter not greater than that of the individual curves in Fig. 12(a). This is true for all tested rods with some deviations which can be explained by errors of measurement. Also shown in Fig. 12(b) are the curves for rods 16 and 15, which have a similar rhombic roughness but less in height.

The transformation by equation (18) was tested by several other data from measurements of rough rods with 2-dim. roughnesses. The scatter of the reduced data was generally less than $\pm 5\%$. From curves as shown in Fig. 12(b) the determination of the Stanton number in different annular flow cross sections is possible if the wall shear stress and hence h^+, are known. The characteristic parameter of each roughness, apart from the roughness geometry, is the ratio of roughness height to the diameter of the rod and tube, respectively, h/d. For the application in a rod bundle, the Stanton number at a certain h^+_{RW}-value can be determined by

$$St = St_0(\gamma^2 - 1)^{-0.3} \quad (19)$$

with the ratio

$$\gamma = r_0/r_1, \quad (20)$$

r_0 being the radius of the equivalent annular zone. This Stanton number must then be transformed by equation (9) to take into account the temperature effect. A further reduction of the Stanton number is possible by

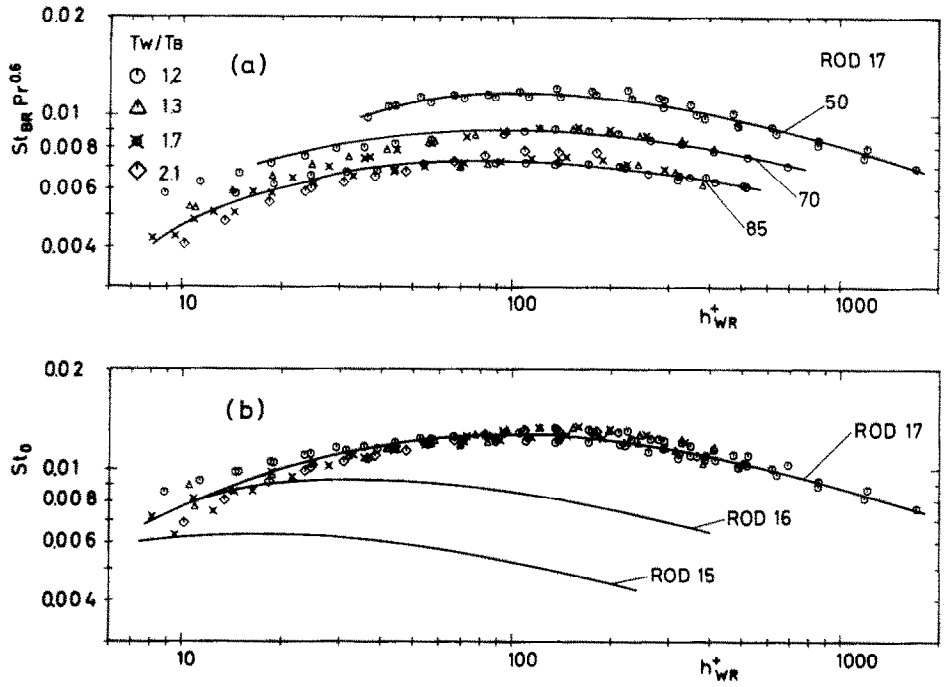

FIG. 12. Stanton numbers for rod 17 in three different outer tubes vs the wall Reynolds number h^+_{WR}, (a) reduced for the temperature effect and (b) transformed to a common flow cross section.

transforming it into a common ratio h/d. Choosing $h/d = 0.01$ we get

$$St_{01} = St_0 \left(\frac{h/r_1}{0.02}\right)^{-0.6}. \tag{21}$$

Contrary to equation (18), this reduction is not valid for all roughnesses, since similarity is not maintained.

For the correlation of St_{01} a new parameter is needed. A suitable one seems to be a transformed roughness Reynolds number

$$Re^* = h^+_{WR}\frac{2r_1}{h} = \frac{u^* d}{\nu_W}\left(\frac{T_W}{T_B}\right)^{0.145}. \tag{22}$$

The results of the transformation by equations (21) and (22) are shown in Fig. 13.

The data of rods 10 and 12 with similar rectangular roughnesses of different heights coincide on one curve. Also, the data of rods 15 and 16, with rhombic roughnesses of different heights, and the data of the small rod 3, with a similar rhombic roughness, lie on a common curve. The data of rod 17 with the extremely high roughness do not agree with the other 'rhombic' data. They are higher at high Reynolds numbers and lower at low Reynolds numbers (not shown). It should be noted that the latter transformation into St_{01} combines roughnesses having the same width and length but different heights, i.e. similarity is not maintained. An extrapolation beyond the tested range of h/d-ratios is not allowed. A comparison with other roughnesses tested at different h/d-ratios is delicate.

Nevertheless, a curve for a two-dimensional roughness with rounded edges ($h/D = 0.015$) measured at small pins in three different outer tubes [43] is shown in Fig. 12. All curves can be correlated by the function

$$St_{01} = a_1 Re^{*m_1} + a_2 Re^{*m_2}. \tag{23}$$

The constants a and m are listed in Table 3 together with the range where the tests were performed.

If the new method is used for calculating the Stanton number and wall temperature, respectively, the knowledge of the roughness parameter G is not necessary, provided that the same h/r_1-ratio is used in the annulus and bundle, or lies in the range given for the validity of equation (23). Since the velocity and temperature profiles are not 'universal', the G parameter cannot be the same for different flow cross sections and different roughnesses. If the roughness parameter G is calculated from the transformed Stanton number St_{01}, we get separate curves for each radius ratio α; lower G for smaller values of α.

THERMAL PERFORMANCES

As mentioned before, the figure of merit for a roughness is the thermal performance $(St_r/St_s)^3/(f_r/f_s)$. The correlations for A_r, R [equation (4) and Table 2] and St_{01} [equation (23)] allow one to calculate the thermal performance of a rod bundle. The Stanton number St_s and friction factor f_s of a smooth tube were calculated by the Dittus–Boelter correlation

$$St_s = 0.023 Re^{-0.2} Pr^{-0.6} \tag{24}$$

and the Prandtl–Nikuradse correlation, respectively

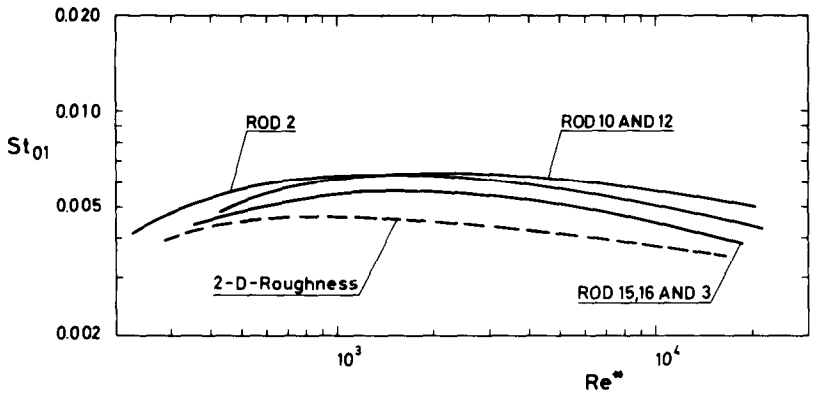

FIG. 13. Comparison of transformed Stanton numbers.

Table 3. Constants of equation (23) for the reduced Stanton number and its range of validity

Rod	a_1	a_2	m_1	m_2	h/d	Re^*
10, 12	0.0312	−0.793	−0.179	−0.816	0.018–0.025	400–2000
15, 16, 3	0.032	−1.79	−0.21	−1.0	0.012–0.025	400–2000
2	0.0221	−3.45	−0.161	−1.191	0.025	200–1000

$$(1/f_s)^{1/2} = 4\log(Ref_s^{1/2}) - 0.4. \quad (25)$$

Figure 14 shows the thermal performance for a 3-dim. roughness in comparison with a 2-dim. trapezoidal roughness for different ratios P/d and a fixed h/d-ratio. For the 3-dim. roughness the parameters of rod 2 were chosen.

The data for the 2-dim. roughness were calculated by the parameter set from [33]

$$\left.\begin{aligned} A_r &= A_H = 2.5 \\ R &= 4.85 \qquad h^+ \geq 60 \\ R &= 7.85 - 1.68\log h^+ \quad h^+ < 60 \end{aligned}\right\} \quad (26)$$

$$GTR1 = 3.28h^{+0.262} + 15/h^+ \quad (27)$$

$$G = GTR1\left(\frac{h/\hat{y}}{0.01}\right)^{0.2}. \quad (28)$$

The friction factor is calculated by equation (5) and the Stanton number by

$$St = \frac{f_{1R}/2Pr^{0.6}}{1 + (f_{1R}/2)^{1/2}[G - R]}. \quad (29)$$

All results are valid for $T_W/T_B = 1$.

This diagram indicates the superiority of the 3-dim. roughness over the 2-dim. one. The maximum value of the thermal performance occurs at different Reynolds numbers. To select an optimum roughness and roughness height, a parametric study must be performed using the correlations given here or elsewhere. Extrapolation to ranges which were not tested should be avoided. Some uncertainty still exists about the dependency of R and especially of G on the h/D_h-ratio, even for 2-dim. roughnesses. Small errors in the Stanton number have a large effect in the value of the thermal performance. Results from the literature are often correlated with $\pm 10\%$ and agreement is claimed with different studies or with theory. For comparing the thermal performance of different roughnesses in a parameter field such data are of little value.

CONCLUSIONS

A parametric study of the drag of 3-dim. roughnesses, the measurement of velocity and temperature profiles over rough surfaces and the measurement of the pressure drop and heat transfer on seven rods with different types of 3-dim. roughnesses in up to four outer tubes gives rise to the following conclusions:

(1) Three-dimensional roughnesses in given p/h- and e/g-ranges produce higher friction factors than 2-dim. roughnesses with the same relative roughness height.
(2) The displacement of the position of zero shear from the surface of maximum velocity in the direction of the smooth wall is larger than for 2-dim. roughnesses.
(3) The 'law of the wall' does neither hold, for the velocity nor for the temperature profile. There is no constant slope for different relative roughness heights. Using constant slopes for the transformation of the friction factor in an annulus leads to errors in f_1 in the order of 5% for large radius ratios ($\alpha = 0.8$) and of 1% for small ones ($\alpha = 0.4$). The application of constant slopes does not yield the same roughness parameter R for different ratios of

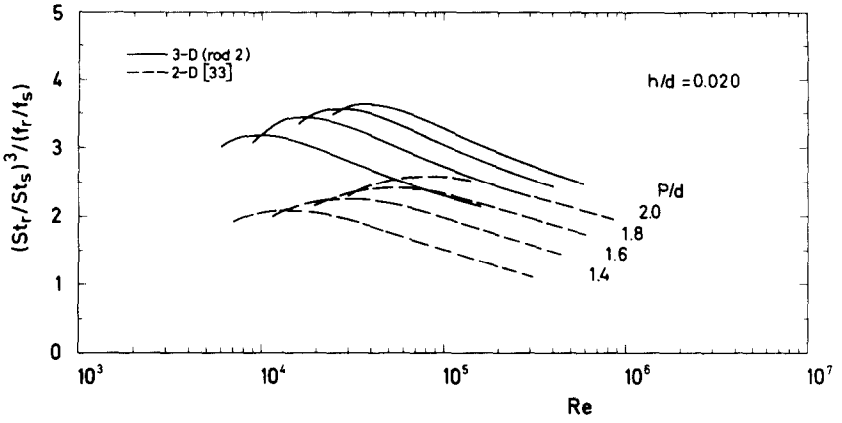

FIG. 14. Thermal performance of rod bundle.

the radius. R- and G-functions can only be used if all conditions of dependence are taken into account.

(4) Any transformation of unsymmetrical into symmetrical rough flow can only give approximate results, the approximation deteriorates with the severity of roughness increasing.

(5) The effect of different wall to gas temperatures on the friction factor and Stanton numbers, can be reduced in most cases, by the same exponents in $(T_W/T_B)^n$ as for 2-dim. roughnesses.

(6) Stanton numbers evaluated from measurements of one rough rod in different outer tubes can be transformed into a common correlation, which is a function of the wall Reynolds number h^+_{WR}, by

$$St_0 = St_{BR}\left(\frac{\alpha^2}{1-\alpha^2}\right)^{-0.3}.$$

Transformation into arbitrary radius ratio is possible by $St = St_0(\gamma^2 - 1)^{-0.3}$.

(7) Three-dimensional roughnesses designed for a high friction factor have a better thermal performance than 2-dim. roughnesses. It is possible, although requiring high manufacturing costs, to obtain the same results on small pins with roughnesses only 0.2 mm high as with large rods.

Acknowledgements—The author wishes to thank Dr M. Dalle Donne, who initiated this program, and all co-workers of the Institute of Neutron Physics and Reactor Engineering of the Karlsruhe Nuclear Research Center who have contributed to the progress of this investigation.

REFERENCES

1. J. Nikuradse, Strömungsgesetze in rauhen Rohren, ForschHft. Ver. Dt. Ing. 361 (1933); NACA TM 1292 (1950).
2. A. E. Bergles and R. L. Webb, Bibliography on augmentation of convective heat and mass transfer, *Previews Heat Mass Transfer* **4**, 89–106 (1978).
3. R. L. Webb, E. R. G. Eckert and R. J. Goldstein, Heat transfer and friction in tubes with repeated-rib roughnesses, *Int. J. Heat Mass Transfer* **14**, 601–617 (1971).
4. R. L. Webb, Toward a common understanding of the performance and selection of roughness for forced convection, in *Studies in Heat Transfer, A Festschrift for E. R. G. Eckert* (edited by T. Irvine *et al.*), pp. 257–272. Hemisphere, Washington, D.C. (1979).
5. M. Dalle Donne and L. Meyer, Turbulent convective heat transfer from rough surfaces with two-dimensional ribs, *Int. J. Heat Mass Transfer* **20**, 583–620 (1977).
6. M. Hudina, Thermohydraulic performance of some ribbed surfaces and their choice for GCFR, *Am. Nucl. Energy* **3**, 351–358 (1976).
7. L. White and D. Wilkie, The heat transfer and pressure loss characteristics of some multi-start ribbed surfaces, in *Augmentation of Convective Heat and Mass Transfer* (edited by A. E. Bergles and R. L. Webb), pp. 55–62. ASME, New York (1970).
8. J. C. Han, I. R. Glicksman and W. M. Rohsenow, An investigation of heat transfer and friction for rib-roughened surfaces, *Int. J. Heat Mass Transfer* **21**, 1143–1156 (1978).
9. D. L. Gee and R. L. Webb, Forced convection heat transfer in helically rib-roughened tubes, *Int. J. Heat Mass Transfer* **23**, 1127–1136 (1980).
10. P. L. Mantle, A new type of roughened heat transfer surface selected by flow visualization technique, *Proc. 3rd Int. Heat Transfer Conf.*, Chicago, Vol. 1, pp. 45–55 (1966).
11. L. Meyer, Turbulente Strömung an Einzel- und Mehrfachrauhigkeiten im Plattenkanal, Kernforschungszentrum Karlsruhe, KfK-Bericht 2764 (1979) and Ph.D. Thesis, University Karlsruhe (1978).
12. W. W. Sayre and M. Albertson, Roughness spacing in rigid open channels, *J. Hydraul. Div. Am. Soc. civ. Engrs* **87** (HY3), 121–150 (1961).
13. D. W. Knight, J. A. Macdonald, Hydraulic resistance of artificial strip roughness, *J. Hydraul. Div. Am. Soc. civ. Engrs* **105** (HY6), 675–690 (1979).
14. M. Dalle Donne and E. Meerwald, Alternate studs: a new type of artificial roughness to improve the performance of a gas-cooled reactor, Proc. 1972 ANS Winter Meeting, *ANS Trans.* **15**, 846–847, Washington (1972).
15. M. Dalle Donne and L. Meyer, Experimental heat transfer and pressure drop at rods with three-dimensional roughnesses in annuli, OECD-NEA Coordinating Group on GCFR Development, Heat Transfer Specialist Meeting, Petten (1975).
16. K. Maubach, Rough annulus pressure drop, Interpre-

tation of experiments and recalculation for square ribs, *Int. J. Heat Mass Transfer* **15**, 2489–2498 (1972); see also: Reibungsgesetze turbulenter Strömungen, *Chemie-Ing.-Technik* **42**, 995–1004 (1970).
17. A. Aytekin, Turbulent flow and heat transfer in channels with combined rough and smooth surfaces, Ph.D. thesis, University of London (1978).
18. A. W. Whitehead, The effect of surface roughening on fluid flow and heat transfer, Ph.D. thesis, University of London (1976).
19. W. Baumann, Geschwindigkeitsverteilung bei turbulenter Strömung an rauhen Wänden, Kernforschungszentrum Karlsruhe, KfK-Bericht 2618 and 2680 (1978) and Ph.D. thesis, University Karlsruhe (1978).
20. L. Meyer, Turbulent flow in a plane channel having one or two rough walls, *Int. J. Heat Mass Transfer* **23**, 591–608 (1980).
21. L. Meyer and L. Vogel, The velocity distribution and pressure loss at artificial roughnesses with sharp and rounded edges, report KfK 2885 (1979).
22. L. Meyer and K. Rehme, Heat transfer and pressure drop measurements with roughened single pins cooled by various gases, report KfK 2980 (1980).
23. L. Meyer, Velocity distribution and pressure loss at three-dimensional roughnesses, report KfK 3026 (1980).
24. L. Meyer, Velocity and temperature profiles in rough annuli, report KfK 3163 (1981).
25. L. Meyer, Heat transfer and pressure drop at single rods with three-dimensional roughnesses: Large scale tests, report KfK 3164 (1981).
26. L. Meyer and W. Neu, Heat transfer and pressure drop at single pins with three-dimensional roughness, report KfK 3165 (1981).
27. M. J. Lewis, An elementary analysis for predicting the momentum and heat transfer characteristics of a hydraulically rough surface, *J. Heat Transfer* **97**, 249–254 (1975).
28. L. Meyer, Flow resistance of rectangular roughnesses with varying density, OECD-NEA Coordinating Group on GCFR-Development, Heat Transfer Specialist Meeting, Würenlingen (1979).
29. D. E. Dipprey and R. H. Sabersky, Heat and momentum transfer in smooth and rough tubes at various Prandtl numbers, *Int. J. Heat Mass Transfer* **6**, 329–353 (1963).
30. F. P. Berger and A. W. Whitehead, Fluid flow and heat transfer in tubes with internal square rib roughening, *J. Br. Nucl. Energy Soc.* **16**, 153–160 (1977).
31. C. Warburton, The interpretation of tests on roughened pins in rough channels and the prediction of cluster pressure drop from single-pin data, C.E.G.B. Report RD/B/N 2930, Berkeley (1973).
32. S. A. Hodge, J. P. Sanders and D. E. Klein, Slope and intercept of the dimensionless velocity profile for artificially roughened surfaces, *Int. J. Heat Mass Transfer* **23**, 135–140 (1980).
33. L. Meyer, Friction and Heat Transfer Correlations for the Roughness of the BR2 Calibration Element, report KfK 2986 (1980).
34. M. Dalle Donne and L. Meyer, Turbulent convective heat transfer from rough surfaces with two-dimensional ribs: transitional and laminar flow, report KfK 2566, EUR 5751e (1978).
35. B. S. Petukhov, U. A. Kurganov and A. I. Gladuntsov, Heat transfer in turbulent pipe flow of gases with variable properties, *Heat Transfer—Sov. Res.* **5**, 109–116 (1973).
36. S. S. Kutateladze, *Fundamentals of Heat Transfer*. Edward Arnold, London (1963).
37. I. T. Alad'yev, Experimental determination of local and mean coefficients of heat transfer for turbulent flow in pipes, NACA TM 1356 (1954).
38. R. Firth, A method of analysing heat transfer and pressure drop data from partially roughened annular channels, UKAEA, Windscale, ND-R-301 (W) (1979).
39. M. Hudina, Evaluation of heat transfer performances of rough surfaces from experimental investigation in annular channels, *Int. J. Heat Mass Transfer* **22**, 1381–1392 (1979).
40. B. Kjellström, Influence of surface roughness on heat transfer and pressure drop in turbulent flow, AE-RTL-819-821, Studsvik (1966).
41. A. C. Rapier, Forced convection heat transfer in passages with varying roughness and heat flux around the perimeter, TRG-report 519 (W), Windscale (1963).
42. W. B. Hall, Heat transfer in channels composed of rough and smooth surfaces, report IGR-TN/W-832, Windscale (1958).
43. S. A. Hodge, L. Meyer, Pressure drop and heat transfer correlations for use in CTFL bundle analysis, report ORNL-PM-7891, Oakridge and KfK 3254, Karlsruhe (1981).

PROPRIETES THERMOHYDRAULIQUES DE BARRES INDIVIDUELLES AUX RUGOSITES A TROIS DIMENSIONS

Résumé—On a étudié les propriétés de transfert de chaleur et de friction de rugosités tridimensionnelles constitutées par protubérances régulièrement distribuées aux arêtes vives. Les résultats de mesures portant sur la distribution de vitesse et de température dans les chambres annulaires rugueuses ont été employés pour évaluer les données résultant de mesures de perte de pression et de transfert de chaleur sur sept barres individuelles aux rugosités différentes placées dans quatre tubes extérieures au maximum. Les résultats montrent que pour des paramètres spécifiques de nervures les rugosités à trois dimensions donnent lieu à des coefficients de friction et à des nombres de Stanton plus élevés que les rugosités à deux dimensions. En présence de ces types de rugosité la loi à la paroi n'est plus valable en ce qui concerne la distribution de vitesse et de température. Sont indiquées dans cette contribution les relations permettant de-déterminer les coefficients de friction et les nombres de Stanton dans différentes chambres annulaires. Une simple méthode est décrite qui permet de transformer les nombres de Stanton obtenus de mesures en chambres annulaires à une section annulaire quelconque.

THERMOHYDRAULISCHE EIGENSCHAFTEN VON EINZELSTÄBEN MIT DREIDIMENSIONALEN RAUHIGKEITEN

Zussammenfassung—Die Wärmeübertragungs- und Reibungseigenschaften drei-dimensionaler Rauhigkeiten, die aus gleichmäßig verteilten Erhebungen mit scharfen Kanten bestehen, wurden untersucht. Ergebnisse von Messungen der Geschwindigkeits- und Temperaturverteilung in rauhen Ringspalten werden benutzt, um Daten aus Druckverlust- und Wärmeübergangsmessungen an sieben verschiedenen rauhen Einzelstäben in bis zu vier glatten Außenrohren auszuwerten. Die Ergibnisse zeigen, daß dreidimensionale Rauhigkeiten mit bestimmten Rippenparametern höhere Reibungsbeiwerte und Stantonzahlen als zwei-dimensionale Rauhigkeiten erzeugen. Bei solchen Rauhigkeiten ist das Wandgesetz für die Geschwindigkeits- und Temperaturverteilung nicht gültig. In diesem Beitrag werden Beziehungen für die Bestimmung von Reibungsbeiwerten und Stantonzahlen in verschiedenen Ringspalten angegeben. Es wird eine einfache Methode beschrieben, die es erlaubt, die Stantonzahlen aus Ringspaltmessungen auf einen beliebigen ringförmigen Querschnitt zu transformieren.

ТЕРМОГИДРАВЛИЧЕСКИЕ ХАРАКТЕРИСТИКИ ОТДЕЛЬНЫХ СТЕРЖНЕЙ С ТРЕХМЕРНЫМИ ШЕРОХОВАТОСТЯМИ

Аннотация — Исследованы характеристики теплоотдачи и гидравлического сопротивления трехмерных шероховатостей, состоящих из равномерно распределенных выступов с острыми краями. Результаты измерений распределения по скоростям и температурам в шероховатых кольцевых зазорах используются для обработки данных, полученных в измерениях гидравлического сопротивления и теплоотдачи на семи различных шероховатых отдельных стержнях, концентрически размещенных в (до четырех) гладких внешних трубах. Результаты показывают, что трехмерные шероховатости с определенными параметрами ребер вызывают более высокие коэффициенты сопротивления трения и числа Стэнтона чем двумерные шероховатости. Для таких шероховатостей закон стенок о распределении по скоростям и температурам не справедлив. В настоящей статье приведены зависимости для определения коэффициентов трения и чисел Стэнтона в различных кольцевых зазорах. Описывается простой метод, позволяющий пересчитывать числа Стэнтона, полученные в измерениях на кольцевых зазорах, на любое кольцеобразное поперечное сечение.